Available online at www.sciencedirect.com
ScienceDirect
Catalysis Communications 9 (2008) 262–268
www.elsevier.com/locate/catcom

Characterization of AC–ZnO catalyst and its photocatalytic activity on 4-acetylphenol degradation

Narayanasamy Sobana, Manickavasakam Muruganandam, Meenakshisundaram Swaminathan *

Department of Chemistry, Annamalai University, Annamalai Nagar 608 002, India

Received 28 January 2007; received in revised form 7 April 2007; accepted 17 April 2007
Available online 13 May 2007

Abstract

The activated carbon–zinc oxide catalysts prepared with different portions of activated carbon (AC) have been characterized by diffuse reflectance spectra (DRS), FT-IR, scanning electron micrograph (SEM), X-ray diffraction (XRD) and BET surface area analysis. Changes in some of the physico-chemical characteristics of ZnO have been observed. It is found that these changes correspond with ZnO surface acid–base property. SEM study reveals a perfect ZnO particle distribution on the AC surface in the catalyst with 9%AC content (9AC–ZnO). Adsorption and photodegradation of 4-AP on 9AC–ZnO are much more higher than bare ZnO. The higher efficiency of this photocatalyst is due to the synergistic effect between ZnO and activated carbon. The catalyst is found to be reusable.

Keywords: Zinc oxide; Activated carbon; SEM; 4-Acetylphenol; Photocatalysis; Synergy effect

1. Introduction

The semiconductor mediated heterogeneous photocatalysis is an interesting and promising technique for environmental cleaning and remediation due to its potential to destroy a wide range of organic and inorganic pollutants at ambient temperatures and pressures. It is also a clean technology in water system treatment, because it uses air and its final decomposed products of organic compounds are harmless products such as CO_2, water and mineral salts. The most effective functional materials used for these processes are nano sized semiconductor oxides like TiO_2 and ZnO [1–10]. Though TiO_2 is the most commonly used effective photocatalyst for a wide range of organic compounds degradation, ZnO is found to be a suitable alternative to TiO_2 since its photodegradation mechanism has been proven to be similar to that of TiO_2 [11]. ZnO has been reported to be more efficient than TiO_2 in some of the process such as the advanced oxidation of pulp mill bleaching wastewater [12], the photooxidation of phenol [13] and photocatalysed oxidation 2-phenyl phenol [14]. Furthermore the optimum pH reported for ZnO process is close to neutral value, whereas the optimum pH for TiO_2 mostly lies in acidic region. Hence the ZnO process is more economical for the treatment of industrial effluents. For practical applications there are some difficulties such as filtration of fine TiO_2/ZnO, fixation of catalyst particles and efficient utilization of UV/sunlight. For these reasons many researchers have been working to increase the efficiencies of these process by modification of catalyst surface. TiO_2 supported on porous materials such as SiO_2, ZrO_2, zeolites and activated carbon were used to increase the adsorption capacity of organic compounds [15–22]. Some authors have reported that the use of inert support increases the decomposition of organic compounds [23–31]. Incorporation of some metals into TiO_2 was also suggested [32–34].

In the present work we report the preparation and characterization of activated carbon–ZnO (AC–ZnO) catalysts and the photocatalytic efficiency of 9AC–ZnO (9%AC) catalyst on the degradation of 4-acetylphenol. Phenols and

* Corresponding author. Tel.: +91 4144 220572.
E-mail address: chemsam@yahoo.com (M. Swaminathan).

1566-7367/$ - see front matter © 2007 Elsevier B.V. All rights reserved.
doi:10.1016/j.catcom.2007.04.040

substituted phenols are highly toxic pollutants present in the aqueous effluents of many chemical industries. The degradation of 4-acetylphenol by TiO_2 has been reported [35].

2. Experimental

2.1. Catalysts preparation

ZnO (surface area 5 $m^2 g^{-1}$, particle size 4.80 μm) was obtained from Merck and used as received. Catalysts with activated carbon (SD fine chemicals – surface area 735.60 $m^2 g^{-1}$, ash content 2.5%, particle size 300 mesh and impurities content of acid soluble (2.5%), water soluble (1.5%)) were obtained by mixing ZnO with activated carbon at different proportions in an aqueous suspension and continuous stirring for 3 h. After this, the mixture was filtered and dried. The catalysts have been denoted as *x*AC–ZnO, where *x* is the activated carbon percentage (w/w) in the solution used for the preparation.

Catalysts with the lower AC contents (4AC–ZnO and 9AC–ZnO) acquire a clear gray color. However, when the AC concentration in the catalysts is increased they become darker. The catalyst with highest AC content (23AC–ZnO) is practically black.

2.2. Equipments

Scanning electron microscopic (SEM) analysis was performed on platinum coated catalysts using a Jeol apparatus model JSM-5610 LV.

A Varian Cary 5E UV/VIS–NIR spectrophotometer equipped with an integrated sphere was used to record the diffuse reflectance spectra (DRS) and to measure the absorbance data of the solution samples. The baseline correction was performed using a calibrated reference sample of barium sulfate. The reflectance spectra of the AC–ZnO catalysts were analyzed under ambient conditions in the wavelength range of 200–800 nm.

The specific surface area of the catalysts was determined through nitrogen adsorption at 77 K on the basis of BET equation using a sorptomatic 1990 instrument.

Powder X-ray diffraction patterns of ZnO, AC and AC–ZnO catalysts were obtained using a Philips PAN analytical X′pert PRO diffractometer equipped with a Cu tube for generating a Cu Kα radiation (wavelength 1.5406 Å) at 40 kV, 25 mA. The particles were spread on a glass slide specimen holder and the scattered intensity was measured between 20° and 85° at a scanning rate of $2\theta = 1.2°$/min at 25° temperature. The digital output of the proportional X-ray detector and the goniometric angle measurements were sent to an online microcomputer for storing and analysis. Peak positions were compared with the standard files to identify the crystalline phases.

FTIR spectrophotometer Thermo Nicolet which has Intel* Pentium II processor with 400 MHz clock speed and 15-in. SVGA monitor with 800 × 600 resolution was used to record IR spectra. The catalysts were incorporated in KBr pellets for the measurements. Water reference spectrum was always subtracted from every spectrum.

2.3. Experimental conditions

Photocatalytic activity of the catalyst was determined by the degradation of 4-acetylphenol in water under UV-irradiation. Hundred milligrams catalyst was added into 50 mL of aqueous solution of 4-AP (3×10^{-4} mol L^{-1}). The solution was irradiated with UV light using Heber multilamp photoreactor model HML-MP 88 which consists of eight medium pressure mercury vapor lamps (8 W) set in parallel and emitting 365 nm wavelength ($I = 1.381 \times 10^{-3}$ einstein L^{-1} s^{-1}). The solution was aerated continuously by a pump to provide oxygen and for complete mixing of reaction solution. To monitor the concentration of 4-AP, 2 mL of the sample was withdrawn at specific time intervals and centrifuged to remove the catalyst. One millilitre of the centrifugate was diluted to 10 mL and its absorbance at 276 nm was measured. Solar light intensity was measured for every 30 min and the average light intensity over the duration of each experiment was calculated. The sensor was always set at the position of maximum intensity. The intensity of solar light was measured using LT Lutron LX-10/A digital Lux meter. The intensity of solar light (1100 × 100 lx) was nearly constant during the experiments. UV spectral measurements were done using Hitachi U-2001 spectrophotometer.

3. Results and discussion

3.1. Surface area measurements

In general, the surface area of the catalyst is the most important factor influencing the catalytic activity. Table 1 lists the BET surface area of the different catalysts. The surface area increases with the increase in AC content. The stoichiometric summation of AC and ZnO areas are quite similar to the one obtained experimentally. In addition to this, the pore volume of the catalysts has been analyzed. As the AC content of catalysts is increased, the pore specific volume also increases. The results seem to indicate that ZnO particles agglomerate on the AC particles without entering into the pores of AC. Under these conditions, the incipient ZnO particles can partially block the pores

Table 1
Surface area and crystallite size measurement

Sample	BET specific surface area ($m^2 g^{-1}$)	Crystallite size (nm)
Bare ZnO	5.05	29.70
4AC–ZnO	13.37	24.38
9AC–ZnO	75.54	22.70
13AC–ZnO	109.94	19.80
23AC–ZnO	176.68	15.23
AC	735.60	4.65

of AC particles, thus reducing the fraction of pores contributed by AC as reported in TiO_2 [36].

Higher specific surface area may be of benefit to their high photocatalytic activity, due to enhanced absorption of photons and adsorption of dye molecules.

3.2. Diffuse reflectance spectral analysis

Fig. 1 shows the UV diffuse reflectance spectra of different AC–ZnO catalysts along with the bare ZnO. Bare ZnO without AC shows a clear absorption edge at around 380 nm and no absorption in visible region is observed. In AC–ZnO catalysts visible light absorption is increased. It is also noticeable from the Fig. 1 that there is no correlation between the AC content and UV spectral change. A similar observation was reported when the semiconductor was immobilized on a polymer [37]. It has been indicated that the increment of surfacial electric charge of oxides by the addition of AC give an absorption increment in the IR region and a color change from white to blue [38]. This color change may be due to the increment of the electric charge in catalysts made of ZnO and AC produced by the acid character increment of the surfacial hydroxyl groups due to the presence of AC.

Absorption spectra of AC–ZnO catalysts may be due to the overlapping of absorption spectrum of AC with ZnO.

3.3. FT-IR study

In order to understand the surface nature, FT-IR spectra were recorded for the ZnO, AC and AC–ZnO catalysts (Fig. 2). FT-IR studies in the region between 4000 and 2500 cm^{-1} determine possible changes in the distribution of hydroxyl groups that could confirm the above mentioned acid–base character modification of the catalysts. In the spectrum of the bare ZnO (Fig. 2a) hydroxyl group

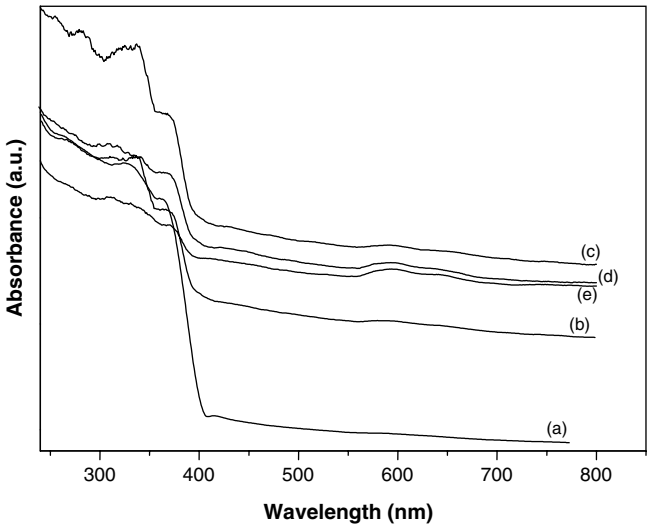

Fig. 1. Diffuse reflectance spectra from the catalysts: (a) bare ZnO; (b) 4AC–ZnO; (c) 9AC–ZnO; (d) 13AC–ZnO; (e) 23AC–ZnO.

Fig. 2. IR spectra from the catalysts: (a) bare ZnO; (b) 4AC–ZnO; (c) 9AC–ZnO; (d) 13AC–ZnO; (e) 23AC–ZnO; (f) AC.

vibration bands are centered at 3449 cm^{-1}. For instance in AC–ZnO catalysts a progressive νOH vibration shift to lower wave numbers (from 3449 to 3399 cm^{-1}) with the increase of AC content of the catalysts is observed (Fig. 2b–e).

These vibration shifts have been attributed to an increment of the positive charge on these OH groups [39] adsorbed on the surface of ZnO confirming the changes of the acid–base character of the hydroxyl groups in these catalysts.

Furthermore, in 800–1600 cm^{-1} region two new bands are obtained. One band at the wavelength of 870–950 cm^{-1} corresponding to C–O–C structure is observed on the surface of AC–ZnO catalysts. The existence of C–O–C structure was confirmed in investigations of basic activated carbon and also in pyrones, which are found to have strong basic sites [40]. Though activated carbon has two broad bands in this region, these bands are structured in AC–ZnO catalysts due to the interaction of ZnO.

3.4. SEM studies

The texture and morphology of the activated carbon, ZnO and AC–ZnO catalysts are very important parameters and might influence the photocatalytic activity. The SEM

image of AC in Fig. 3a depicts that the crystallinity is more in activated carbon and the surface of the carbon is irregular and not spherical as expected. The SEM image of ZnO (Fig. 3b) confirms that zinc oxide presents a porous, sponge like network. It is found that in 9AC–ZnO (Fig. 3d) the AC particles are homogeneously covered by ZnO particles, which agrees with the previous results [35]. In contrast, in the catalysts with higher AC contents i.e., 13AC–ZnO (Fig. 3e) and 23AC–ZnO (Fig. 3f) small ZnO conglomerates are dispersed among large and small AC particles and many of them are not covered by ZnO.

3.5. XRD analysis

Fig. 4 shows X-ray diffraction patterns for bare ZnO, AC and some AC–ZnO crystallites with a different content of AC. All catalysts (Fig. 4a–e) exhibit only patterns assigned to the well crystalline hexagonal phase of ZnO. As the AC content in AC–ZnO catalysts is increased, a small peak at $2\theta = 44.6°$ emerges. This peak corresponds to AC, which is present in 100% relative intensity in the XRD pattern of AC (Fig. 4f). The gradual increase in the intensity and sharpness of the peak at $2\theta = 44.6°$ of AC clearly illustrates the increase in the loading of AC. AC crystallinity is enough to allow its detection at the concentration above 4%AC in the catalyst.

The crystal size was determined from the diffraction peak broadening employing the following equation:

$$D = \frac{K\lambda}{(\beta_c - \beta_s)\cos\theta}$$

where D is the crystal size of the catalyst, λ is the X-ray wavelength, β_c and β_s are the FWHM of the catalyst and the standard, respectively. K (0.89) is a coefficient and θ

Fig. 3. Scanning electron micrograph image from (a) AC; (b) bare ZnO; (c) 4AC–ZnO; (d) 9AC–ZnO; (e) 13AC–ZnO; (f) 23AC–ZnO catalysts.

Fig. 4. XRD patterns from (a) bare ZnO; (b) 4AC–ZnO; (c) 9AC–ZnO; (d) 13AC–ZnO; (e) 23AC–ZnO; (f) AC catalysts.

is the diffraction angle. The values are given in Table 1. The crystal size of bare ZnO decreases from 29.70 nm by the addition of AC. These observations are consistent with the values of surface area.

3.6. Adsorption of 4-acetylphenol

Fig. 5a shows a plot of BET surface area of AC–ZnO catalyst against the carbon content of AC–ZnO catalysts. Content of carbon is directly proportional to the BET surface area of the prepared catalysts, because the BET surface area of AC–ZnO catalysts is related mainly to the amount of carbon. In Fig. 5b, the 4-AP adsorption capacity of catalysts versus content of carbon is plotted. Fig. 5c gives the adsorption capacity of 4-AP against the BET surface area of the catalysts. Adsorption of 4-AP increases with the increase of BET surface area as expected.

3.7. Photocatalytic degradation of 4-acetylphenol

Based on the results obtained from the characterization of the catalysts, we have chosen 9AC–ZnO for the photocatalytic degradation of 4-AP. The result of photocatalytic degradation of 4-AP is shown in Fig. 6. It is observed first that the direct photolysis without solids can be neglected as there is only 3% degradation within 180 min of UV-irradiation. A period of adsorption in the dark of 30 min has been chosen for the attainment of adsorption equilibrium. The degradation of 4-AP in the presence of UV-irradiated AC is quite negligible with less than 7% after 150 min of UV-irradiation. Bare ZnO gives a complete disappearance of 4-AP in about 240 min of UV-irradiation. By contrast 9AC–ZnO totally eliminates 4-AP from the solution within 150 min.

With activated carbon, removal of 4-AP from its aqueous solution observed is only due to adsorption, because it does not have any photoactivity. On AC–ZnO catalysts,

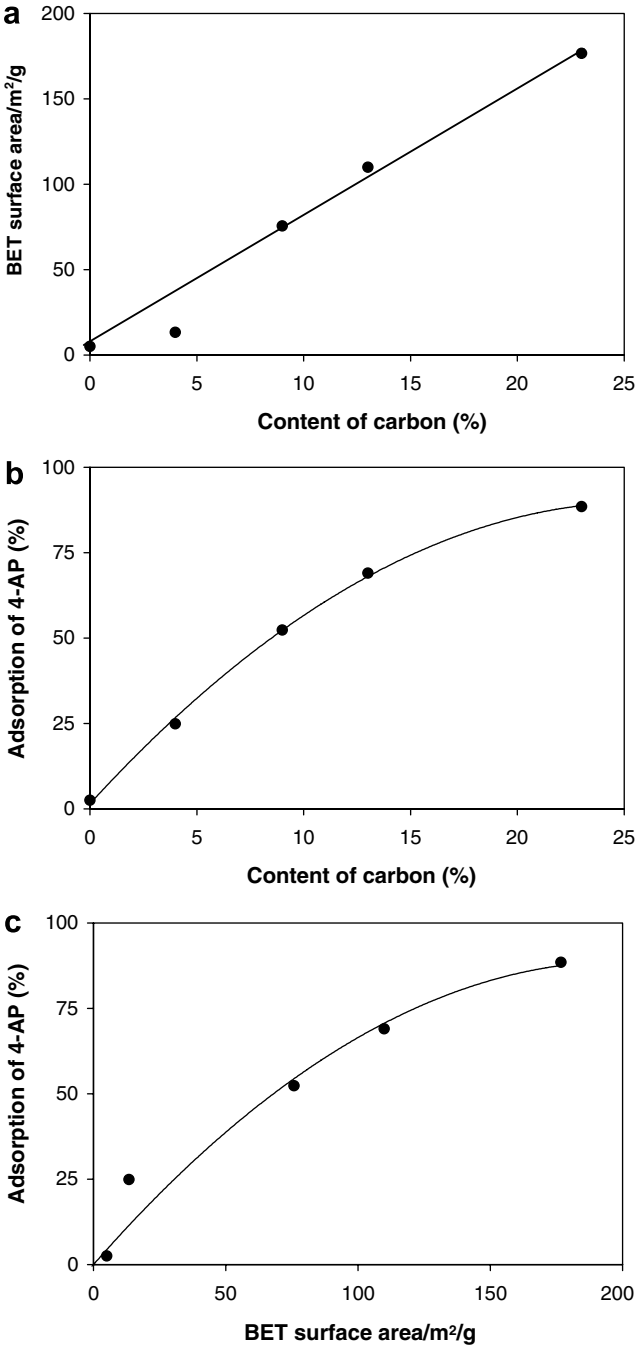

Fig. 5. Dependence of: (a) BET surface area on content of carbon; (b) adsorption of 4-AP on the content of carbon; (c) adsorption of 4-AP on BET surface area, for bare ZnO and AC loaded ZnO catalysts.

both processes, adsorption of 4-AP by activated carbon and its degradation by ZnO photocatalysts, occur at the same time. Since the adsorption process onto activated carbon proceeds much faster than the degradation by the photocatalysis, the removal of 4-acetylphenol in the first 40 min occurs mainly by the former process. Gradual increase in removal of 4-AP after 40 min is by both processes, i.e. adsorption and degradation [24].

A plot of $\ln C_0/C$ versus time of irradiation for ZnO and AC–ZnO shows linearity. The linear transforms

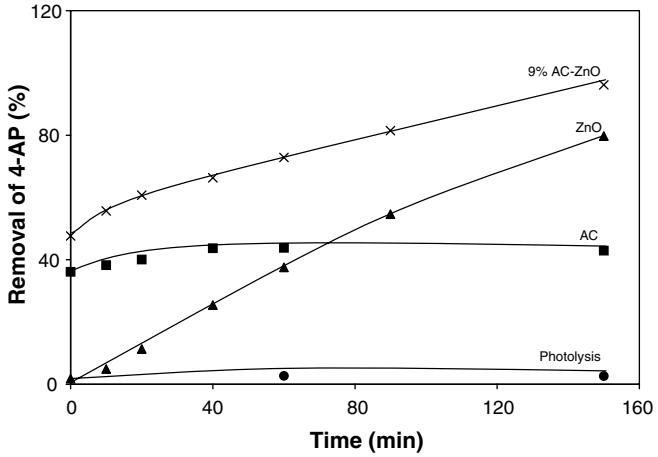

Fig. 6. Kinetic curves of 4-AP disappearance in the presence of various illuminated solids during UV-irradiation.

$\ln C_0/C = f(t)$ of the kinetic curves 4AP disappearance are shown in Fig. 7. This reveals that the reaction is of apparent first order. The apparent rate constants k for 4-acetylphenol photodegradation calculated for ZnO and 9AC–ZnO are

$$\mathrm{ZnO} : k_{\mathrm{app}} = 1.064 \times 10^{-2}\ \mathrm{min}^{-1}$$

$$9\mathrm{AC} - \mathrm{ZnO} : k_{\mathrm{app}} = 2.12 \times 10^{-2}\ \mathrm{min}^{-1}$$

The photocatalytic activity of 9AC–ZnO system determined from the rate constant is higher than that of bare ZnO. The apparent rate constant has been generally chosen as the basic kinetic parameter for the different systems, since it is independent of the concentration. It enables one to determine a photocatalytic activity independent of the previous adsorption period in the dark and of the concentration of 4-AP remaining in the solution. Since AC–ZnO absorbs more sunlight when compared to bare ZnO, the degradation of 4AP was carried out with AC–ZnO using UV and solar light and the results are shown in Fig. 8. It is found that AC–ZnO is more efficient in solar light than in UV light. A complete degradation of

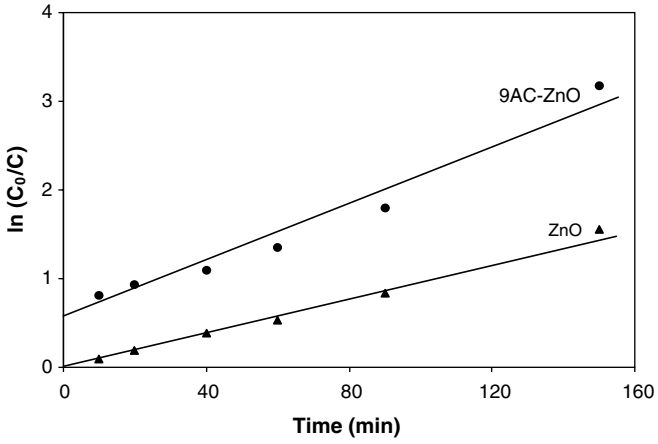

Fig. 7. Apparent first order linear transform $\ln C_0/C = f(t)$ of the kinetic curves of 4AP disappearance for ZnO and AC–ZnO.

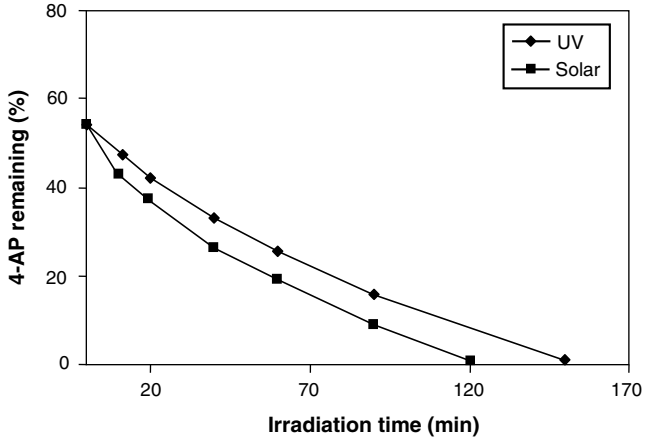

Fig. 8. Comparison of UV and solar irradiation of 4-AP (3×10^{-4} mol L^{-1}) using 9AC–ZnO catalyst.

3×10^{-4} mol L^{-1} with solar light is observed in 120 min, which is less than the time for complete degradation (150 min) in UV light.

3.8. Synergy effect

The following observations reveal that the higher efficiency in the degradation by AC–ZnO than ZnO is mainly due to the synergistic effect between ZnO and activated carbon in aqueous suspension. (i) Before irradiation, the AC–ZnO mixture has adsorbed much more 4-AP in the dark than ZnO alone. (ii) After irradiation 4-AP free water has been obtained with AC–ZnO. This shows that the extended adsorption of 4-AP on AC is followed by a transfer to ZnO where it is photochemically degraded.

This synergistic effect is also revealed by FT-IR studies. Fig. 9a and b shows FT-IR spectra of AC–ZnO photocatalyst before and after complete adsorption of 4-AP in dark. FT-IR spectrum in Fig. 9b shows the characteristic peaks of 4-AP. This indicates the adsorption of 4-AP on the AC–ZnO catalyst. The FT-IR spectrum of AC–ZnO photocatalyst after the complete degradation is shown in Fig. 9c. Comparison of Fig. 9b and c reveals that the characteristic peaks of 4-AP on the absorption spectra of AC–ZnO present in Fig. 9b disappeared and the spectrum in Fig. 9c is similar to the spectrum of the catalyst given in Fig. 9a. So the 4-AP molecules adsorbed on AC–ZnO has been completely degraded. This indicates that the substrate 4-AP, adsorbed on AC is being transferred to the ZnO present in the pores where they are degraded under irradiation. The synergy factor estimated quantitatively from the ratio of apparent rate constants of ZnO and AC–ZnO is around 2.

To simulate the recycling of AC–ZnO catalyst and to confirm the synergistic effect, the prepared AC–ZnO catalyst was repeatedly used. The sample of photocatalyst was kept first in the dark for 30 min to saturate the adsorption of 4-AP and then exposed to UV radiation (first cycle). After 150 min, the sample was separated from the test solution by filtering and then dispersed again into a virgin

Fig. 9. FT-IR spectra of (a) fresh AC–ZnO, (b) AC–ZnO after 4-AP adsorption and (c) AC–ZnO after complete degradation of 4-AP.

solution with the same concentration, being again kept in the dark for about 30 min and then irradiated by UV light for 150 min (second cycle). There is slight difference in adsorption on activated carbon between the first and second cycles. This may be due to the higher adsorption of 4-AP on a clean surface in the first cycle. But the rates of 4-AP removal in both cycles are similar. After 150 min of irradiation, the amounts of 4-AP remaining in the first and second cycles are 1.77% and 2.30%, respectively.

4. Conclusions

In the catalysts with AC content lower or equal to 9% in weight ZnO particles do not form conglomerates, but get adsorbed on the AC particles surface. The distribution of ZnO is found to be more homogeneous in 9AC–ZnO when compared to other AC–ZnO catalysts. On UV-irradiation bare ZnO gives a complete removal of 4-acetylphenol in 240 min whereas 9AC–ZnO degrades completely in 150 min. 9AC–ZnO is found to be more efficient in solar light than in UV light. The higher efficiency of this photocatalyst is due to the synergistic effect between ZnO and activated carbon. The synergy factor is found to be two. The efficiency of the catalyst is stable and it is reusable.

References

[1] E. Evgenidou, K. Fytianos, I. Poulios, Appl. Catal. B. Environ. 59 (2005) 83.
[2] N. Daneshvar, D. Salari, A.R. Khataee, J. Photochem. Photobiol. A. 162 (2004) 317.
[3] A.A. Khodja, A. Boulkamh, C. Richard, Appl. Catal. B. Environ. 59 (2005) 151.
[4] I.K. Konstantinou, T.A. Albains, Appl. Catal. B. Environ. 49 (2004) 1.
[5] V. Kandavelu, H. Kastien, K. Ravindranathan Thampi, Appl. Catal. B Environ. 48 (2004) 101.
[6] M. Muruganandam, M. Swaminathan, Sol. Energy Mater. Sol. Cells 81 (2004) 439.
[7] M. Muruganandam, M. Swaminathan, Dyes Pigments 62 (2004) 271.
[8] M. Muruganandam, M. Swaminathan, Dyes Pigments 63 (2004) 315.
[9] M. Muruganandam, M. Swaminathan, Dyes Pigments 68 (2006) 133.
[10] C. Lizama, J. Freer, J. Baeza, H.D. Mansilla, Catal. Today 76 (2002) 235.
[11] B. Dindar, S. Icli, J. Photochem. Photobiol. A: Chem. 140 (2001) 263–268.
[12] M.C. Yeber, J. Roderiguez, J. Freer, J. Baeza, N. Duran, H.D. Mansilla, Chemosphere 39 (1999) 10–16.
[13] A.A. Khodja, T. Sheili, J.F. Pihichowski, P. Boule, J. Photochem. Photobiol. A: Chem. 141 (2001) 231–239.
[14] N. Serpone, P. Maruthamuthu, P. Pichat, E. Pelizzetti, H. Hidaka, J. Photochem. Photobiol. A: Chem. 85 (2001) 247–253.
[15] J. Matos, J. Laine, J.M. Herrmann, Appl. Catal. B: Environ. 18 (1998) 281.
[16] H.-R Chen, J.L. Shi, W.H. Zhang, M.L. Ruan, D.S. Yan, Chem. Mater. 13 (2001) 1035.
[17] M. Hirano, C. Nakahara, K. Ota, M. Inagaki, J. Am. Ceram. Soc. 85 (2002) 1333.
[18] J.M. Herman, H. Tahiri, G. Ait-Ichou, G. Lassaletta, A.R. Gonzalez-Elipe, A. Fernandez, Appl. Catal. B 13 (1997) 219.
[19] T. Tsumura, N. Kojitani, H. Umemura, M. Toyoda, M. Inagaki, Appl. Surf. Sci. 196 (2002) 429.
[20] J. Matos, J. Laine, J.M. Herrmann, J. Catal. 200 (2001) 10.
[21] Z. Ding, G.Q. Lu, P.F. Greenfield, J. Colloid Interf. Sci. 232 (2000) 1.
[22] J. Chen, L. Eberlin, C.H. Langford, J. Photochem. Photobiol. A 148 (2002) 183.
[23] B. Tryba, A.W. Morawski, T. Tsumura, M. Toyoda, M. Inagaki, J. Photochem. Photobiol. A 167 (2004) 127.
[24] B. Tryba, A.W. Morawski, M. Inagaki, Appl. Catal. B 46 (2003) 203.
[25] S.A. Carabineiro, F.B. Fernandez, J.S. Vital, A.M. Ramos, I.M. Fonseca, Appl. Catal. B 59 (2005) 185.
[26] B. Tryba, A.W. Morawski, M. Inagaki, Appl. Catal. B 41 (2003) 427.
[27] H. Yoneyama, T. Torimoto, Catal. Today 58 (2000) 133.
[28] G. Colon, M.C. Hidalgo, M. Macias, J.A. Navio, J.M. Dona, Appl. Catal. B 43 (2003) 163.
[29] B. Tryba, T. Tsumura, M. Janus, A.W. Morawski, M. Inagaki, Appl. Catal. B 50 (2004) 177.
[30] J. Arana, J.M. Dona-Rodriguez, C. Garria i Cabo, O. Gonzaliz-Diaz, J.A. Herrera-Melian, J. Perez-Pena, Appl. Catal. B 53 (2004) 221.
[31] E. Carpio, P. Zuniga, S. Ponce, J. Solis, J. Rodriguez, W. Estrada, J. Mol. Catal. A Chem. 228 (2005) 293.
[32] S. Kato, Y. Hirano, M.I. Wata, T. Sano, K. Takeuchi, S. Matsuzawa, Appl. Catal. B 57 (2004) 109.
[33] J. Arana, C. Garriga i Cabo, J.M. Dona-Rodriguez, O. Gonzalez-Diaz, J.A. Herrera-Melian, J. Perez-Pena, Appl. Surf. Sci. 239 (2004) 60.
[34] K.T. Ranjit, B. Viswanathan, J. Photochem. Photobiol. A 108 (1997) 79.
[35] K.E. O'Shea, Claudia Cardona, J. Org. Chem 59 (1994) 5005.
[36] J. Arana, J.M. Dona-Rodriguez, E. Tello Rendon, E. Garriga i Cabo, O. Gonzalez-Diaz, J.H. Herrera-Melian, J. Perez-Pena, G. Colon, J.A. Navio, Appl. Catal. B 44 (2003) 161.
[37] V. Brezova, M. Jankovicova, M. Soldan, A. Blazkova, M. Rehakova, I. Surina, M. Ceppan, B. Havilinova, J. Photochem. Photobiol. A 83 (1994) 69.
[38] I. Bedja, S. Hotchandani, P.V. Kamat, J. Phys. Chem. 97 (1993) 11064.
[39] P.H. Conner, K.D. Dobson, A.J. McQuillan, Langmuir 15 (1999) 2402.
[40] J.E. Papirer, S. Li, J.B. Donnet, Carbon 25 (1987) 243.